Research Article

Fly ashes as a sustainable source for nanostructured Si anodes in lithium-ion batteries

An Xing[1] · Jun Zhang[1] · Ruzhuan Wang[1] · Jun Wang[1] · Xiaoyan Liu[1]

Abstract
Recycling industrial wastes for high-value items is of strategic importance for commercial production. Fly ashes are solid waste by-products generated by coal-fired power plants. Although a large amount of annual output approach 150 million tons worldwide, fly ashes have been recycled merely into some low-value items. In order to realize the high additive value of fly ashes, we transform the solid waste fly ashes into nanostructured silicon powders and apply them as anodes active materials for lithium-ion batteries. The nanostructured silicon exhibits good electrochemical performance as lithium-ion batteries anodes with high rate capacity (1450.3 mAh g^{-1} at current density 4000 mA g^{-1}) and reversible capacity (1017.5 mAh g^{-1} after 100 cycles), indicating that fly ashes can be a useful resource of anode materials to meet the need of high performance lithium-ion batteries.

Keywords Fly ashes · Nanostructured Si · Anodes · Lithium-ion batteries

1 Introduction

Fly ashes are solid waste by-products generated by coal-fired power plants, and the yield of fly ashes approach 150 million tons/year worldwide in 1990 [1]. Moreover, the increasing energy demands of developing countries is possible to ensure that the coals are key components of energy consumption despite the climate-change policy [2, 3]. As a result, it can be expected that the amount of fly ashes will increase with the energy demand increases in the future. The super yield of waste by-products results in an environmental issue inevitably, hence, the comprehensive utilization of this solid waste resources is closely related to global sustainable development strategy. However, less than a half of the solid waste fly ashes are recycled for concrete, cement and as a solid additive, and they are mainly used in a narrow range of low-value items [4]. The remainder still being directly discharged into fly ashes ponds and landfills leading to various environmental problems [5]. Typically fly ashes are composed primarily of aluminosilicate glass, mullite ($Al_6Si_2O_{13}$) and quartz (SiO_2), and they can provide a ready source for Si and Al, which are necessary for the preparation of zeolites [6]. In this context, some valuable applications are focus on the conversion of fly ashes to zeolites [7, 8], solid catalyst [9, 10], porous materials [11] and adsorption of textile dyes to data [12, 13]. However, other more valuable applications must be investigated to enhance the value of the fly ashes and to recycle the high fly ashes output.

It is well known that Si have important industrial and potential applications in the field of high technology, such as semiconductor [14], nanoelectronic [15], biotechnology [16–18], and energy storage [19–22]. In these applications, Si has aroused considerable attention as the alternative lithium-ion batteries anode materials for portable electronic devices and electric vehicles on account of its large

Electronic supplementary material The online version of this article (https://doi.org/10.1007/s42452-019-0196-y) contains supplementary material, which is available to authorized users.

✉ An Xing, devid14@163.com | [1]Chongqing Key Laboratory of Nano-Micro Composite Materials and Devices, School of Metallurgy and Materials Engineering, Chongqing University of Science and Technology, Chongqing 401331, China.

SN Applied Sciences (2019) 1:181 | https://doi.org/10.1007/s42452-019-0196-y

Received: 7 August 2018 / Accepted: 21 January 2019 / Published online: 25 January 2019

theoretical specific capacity (4200 mAh g^{-1} for $Li_{4.4}Si$), which can be up to ten times greater than that of conventional graphite anode (370 mAh g^{-1}) [19, 23–25]. However, the giant volume changes (> 300%) is caused by the process of lithium insertion and extraction, which lead to the fracture and pulverization of Si structure [26]. As a result, Si typically suffers a severe capacity fading during cycling. Many research works have shown that nanostructured Si can effectively accommodate such volume changes and significantly improve the cyclic performance [19–22, 27–29], nevertheless, the high cost of nanostructured Si production is a restricted facror for Si anodes compared to graphite anodes. Therefore, an increased interest has been noted lately in the use of low-cost waste products (rice husks and reed plants) as Si sources for the preparation of nanostructured Si anodes [30–33]. However, the research on how to extract the nanostructured Si out from solid waste fly ashes generated by coal-fired power plants is paid less attention [34]. Considering this, current work explores the expensive nanostructured Si materials can be easily produced from coal-fired power wastes present in abundance by a green and economical approach.

2 Experimental

2.1 Materials

In a typical synthesis, the industrial fly ashes were used as the Si source. The raw fly ashes materials were obtained from a coal-fired electric power station in China. Mg powders (250 mesh) were obtained from Aladdin Reagent, China. For comparison with the derived Nano-Si from fly ashes, Si powders (6000 mesh) were obtained from a commercial vendor (CNPC Powder Material Co., China).

In order to realize the high additive value of fly ashes, in this work, we transform the solid waste fly ashes into nanostructured silicon (Nano-Si) powders and apply them as anodes active materials for lithium-ion batteries.

The optical images and flow chart are shown in Fig. 1a–e, solid waste fly ashes are first transformed into nanostructured SiO_2 (Nano-SiO_2) by thermal treatment with alkali fusion and water bath, in the next section the Nano-Si is synthesized through magnesiothermic reduction. Finally electrochemical properties of the Nano-Si as anodes for LIBs are examined.

2.2 Synthesis of Nano-SiO_2 from fly ashes

To increase its activity in Nano-SiO_2 formation, firstly, fusion of fly ashes powders with Na_2CO_3 was carried out at 800 °C for 2 h (1:0.8 fly ashes:Na_2CO_3 weight ratio), and the resultant fused mixture was then cooled down to the room temperature. After that, the product of fusion was leached with a 3 M HCl solution for 4 h in order to eliminate some metal ions. The leached product of fusion was washed with deionized water to neutral conditions, then heated in water bath at 100 °C for 6 h, then the Nano-SiO_2 was collected by filtration to remove aluminium oxide, and dried at 105 °C.

2.3 Transformation of Nano-SiO_2 to Nano-Si

300 mg of the synthesized Nano-SiO_2 was fully mixed up with 300 mg of Mg powders. The mixture was spread evenly in a steel boat, then heated to 650 °C for 5 h inside a tube furnace under 95 vol% Ar/5 vol% H_2 gas flow. The

Fig. 1 Nano-Si extraction from solid waste fly ashes generated by coal-fired power plants in a green and economical approach. **a** Fly ashes generated by coal-fired power plants. **b** Process flow diagrams of the transformation from fly ashes to Nano-Si powders. R.T. denotes room temperature. **c**–**e**, Optical images of the intermediate substances

ramp rate was controlled at 5 °C min^{-1}. After this reduction, the obtained dark brown powders were soaked in 2 M hydrochloric acid (HCl) aqueous solution for 12 h to selectively remove MgO and Mg_2Si, and then treated in a 5 wt% HF solution for 5 min to insure that newly formed or any unreacted SiO_2 was eleminated. The resultant Nano-Si powders were gathered by filtration, cleaned with de-ion water and absolute ethanol for 4 times, respectively, and finally dried under vacuum at 80 °C for 6 h.

2.4 Characterization

XRD spectra were acquired at room temperature with a Rigaku SmartLab 9 diffractometer using Cu Kα radiation (40 mA, 40 kV) to analyze the structure of crystals. The morphologies of all materials were characterized by FESEM (JEOL JSM-7800F) and HRTEM (JEOL JEM-2100F). The EDS attached to TEM and SEM apparatus was served as elemental analysis. The nitrogen adsorption–desorption isotherm was acquired through the Brunauer–Emmett–Teller (BET) (Micrometrics ASAP 2020 analyzer) after vacuum degas of the samples at 200 °C for 3 h.

2.5 Electrochemistry

To obtain the Nano-Si working electrodes, the slurry was prepared by dissolving 10 wt% sodium alginate, 10 wt% Super P, and 80 wt% Nano-Si in water. The slurry was cast onto thin copper foils. The coated electrodes were heated in a vacuum oven at 75 °C for 12 h, and then they were punched into circular discs to fabricate the coin-cell. The load of active materials was about 1.2 mg/cm^2. The electrolyte used in the current study is 1.0 M $LiPF_6$ in the mixture of carbonates (Novolyte Technologies Inc. Suzhou, China). For electrochemical evaluation, coin-type cell (CR2016) was assembled by sandwiching separator (Celgard 2400) with the Nano-Si working electrode and the metal Li metal counter electrode inside the glove box. The cell was charged and discharged galvanostatically in a fixed voltage window from 5 mV to 1.0 V on a LAND battery test system (Wuhan Kingnuo Electronics Co., Ltd., China) at 25 °C. Cyclic voltammogram (CV) was conducted on an Autolab PGSTAT302 N workstation by 0.02 mV s^{-1} scan.

3 Results and discussion

The fly ashes used in the present study were gathered from a coal-fired power plant in China during July 2017 (Fig. 1a, c). Chemical composition of the raw fly ashes used in the current research are showed in Table S1. Characterization by scanning electron microscopy (SEM) indicated that the fly ashes typically are agglomerate of spheres about 1–100 μm in diameter (Fig. S1a). Moreover, an X-ray diffraction pattern (XRD) exhibited that fly ashes are mainly composed of mullite ($Al_6Si_2O_{13}$) and quartz (SiO_2) (Fig. S1b). The solid waste fly ashes are first converted to Nano-SiO_2 by thermal treatment with alkali fusion and water bath, the detailed synthetic step are summarized in Fig. 1b. The elemental analysis with energy dispersive spectroscopy (EDS) indicated that the fly ashes indeed are converted to SiO_2 (Figs. 1d and S2) after the thermal treatment with alkali fusion and water bath, suggesting that most other components were leaved out (such as Al^{3+}, Fe^{3+}, Ca^{2+}, Mg^{2+}, Na^{+}) (Table S1), and the XRD pattern also showed amorphous nature of the SiO_2 (Fig. 2c). Figure 2a, b showed SEM images of Nano-SiO_2 derived from fly ashes under low and high magnifications. The images clearly confirmed that nanoporous structure is obtained, which is attributed to the acid etching of the metal oxide components in fly ashes. Such changes were reflected in the increase of the specific surface area (3.9 → 38.2 m^2 g^{-1}, Figs. S1c,2d). The porosity measurements further supported for the porous nature of Nano-SiO_2 (Fig. 2d). N_2 adsorption–desorption experiment exhibited an isotherm that was the IV type containing an apparent hysteresis loop at higher relative pressures (P/P_0), which indicated that the derived SiO_2 from fly ashes are porous materials.

Meanwhile, the peaks between 5 nm and 20 nm according to the pore-size distribution of the Barrett-Joyner-Halenda (BJH) further proves the main presence of mesopores (Fig. 2d inset). Next, the derived Nano-SiO_2 was reduced to acquire Nano-Si through a magnesiothermic reduction.

In an effort to transfer the fly ashes-derived Nano-SiO_2 to Nano-Si, magnesium powders (b.p. = 650 °C) were used as reducing agents, Nano-SiO_2 and Mg powders were mixed thoroughly at the rate of 1:1 in mass, and then the magnesiothermic reduction occured at 650 °C for 7 h in 5 vol% H_2-95 vol% Ar gas flow. X-ray diffraction (XRD) patterns of the products synthesized through magnesiothermic reduction of fly ashes-derived SiO_2 before acid etching showed that the sample had sharp peaks from Si-MgO mixture including Si, MgO and Mg_2Si (Fig. 3a). The fly ashes-derived SiO_2 was transferred to the Si-MgO mixture with the magnesiothermic reduction as below [35]:

$$SiO_2\,(s) + 2Mg\,(g) \rightarrow Si\,(s) + 2MgO\,(s)$$

If Mg is excess in the reaction,

$$2Mg\,(g) + Si\,(s) \rightarrow Mg_2Si\,(s)$$

The products including the MgO and Mg_2Si were selectively removed and the yellow–brown crystalline Si material was acquired which was confirmed through XRD patterns (Fig. 3b) and optical images (Fig. 1e).

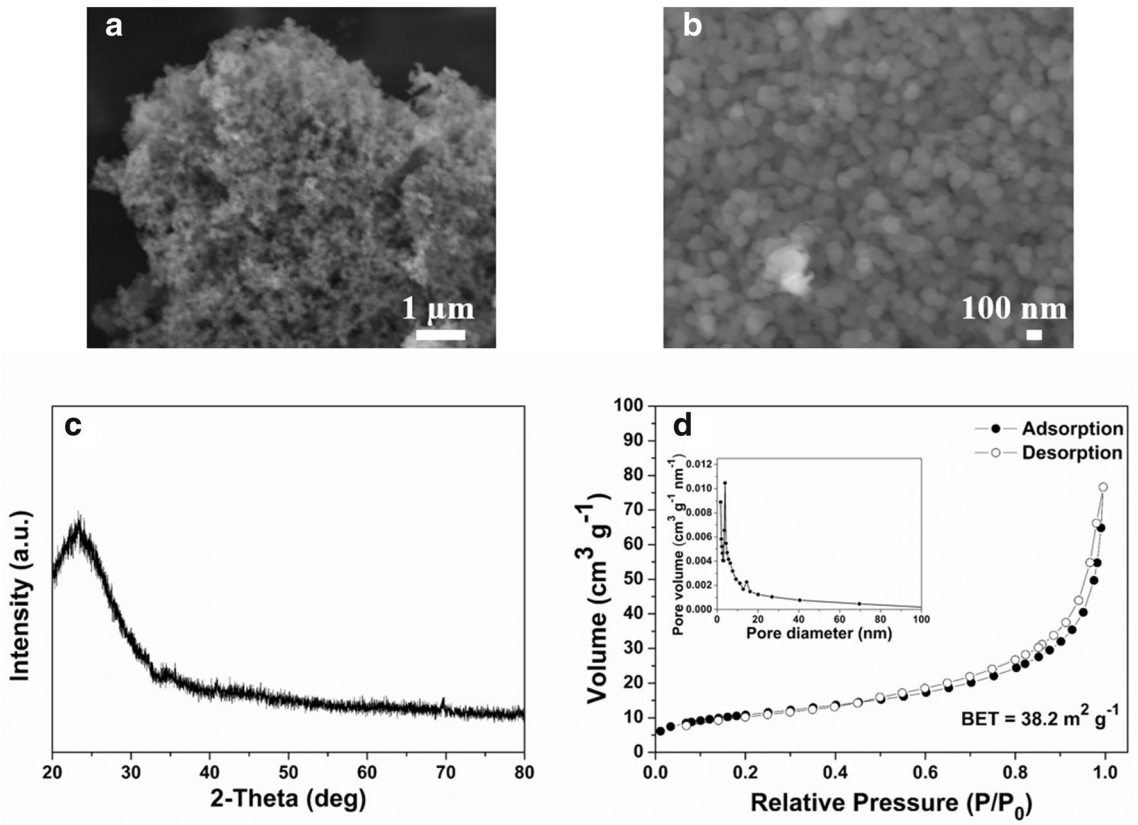

Fig. 2 Characterization of Nano-SiO_2 obtained from fly ashes. **a**, **b** SEM images of Nano-SiO_2 derived from fly ashes. **c** XRD pattern of the SiO_2 derived from fly ashes. **d** N_2 adsorption–desorption isotherms of Nano-SiO_2 derived from fly ashes. Inset, pore distribution

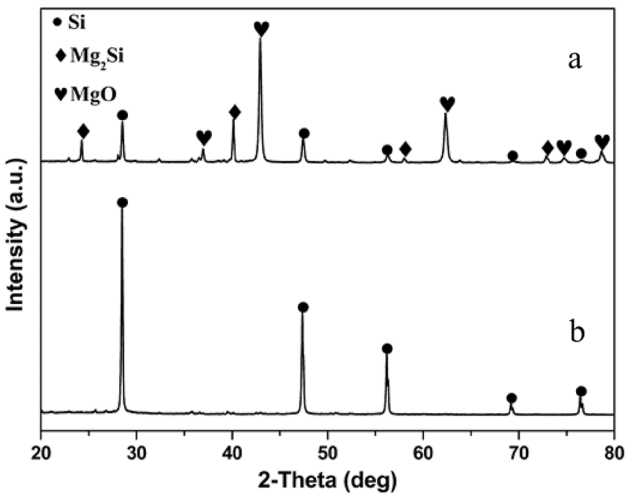

Fig. 3 X-ray diffraction patterns of products synthesized through magnesiothermic reduction of fly ashes-derived Nano-SiO_2. a, XRD patterns of Si-MgO mixture. b, XRD patterns of Si samples treated with HCl/HF etching

Furthermore, the fine crystalline Si was also verified with high resolution transmission electron microscopy (HRTEM, Fig. 4c). The lattice spacing of the crystalline Si is shown in the higher magnification TEM image, which matches the (111) planes of the silicon (Fig. 4c). However, the TEM image of the Nano-Si powders (Fig. 4b) further indicated that crystalline Si nanoparticles were dispersed over the amorphous Si matrix, and we can infer that the amorphous Si matrix will act as a buffer layer which can help alleviate the volume changes and improve the electrochemical performance. The porous structure of Nano-Si products was not observed obviously with the secondary electron microscopy (SEM) image (Fig. 4a). The pore size distribution and surface area of Nano-Si products were appraised with N_2 adsorption–desorption experiment. The N_2 adsorption and desorption curve of Nano-Si products was the IV type containing a hysteresis loop of H1 type (Fig. 4d). The result indicated that Nano-Si products were also porous, which was in accordance with the analysis of pore diameter (Fig. 4d inset). However, the porous structure of derived Nano-Si was transformed into the interconnected porous structure (Fig. 4b), and this transformation was also present on the decrease of the specific surface area ($38.2 \rightarrow 13.3\ m^2\ g^{-1}$, Figs. 2d, 4d). This could be due to the removal of Si-MgO mixture and the growth of grains treated with acid etching and high temperature.

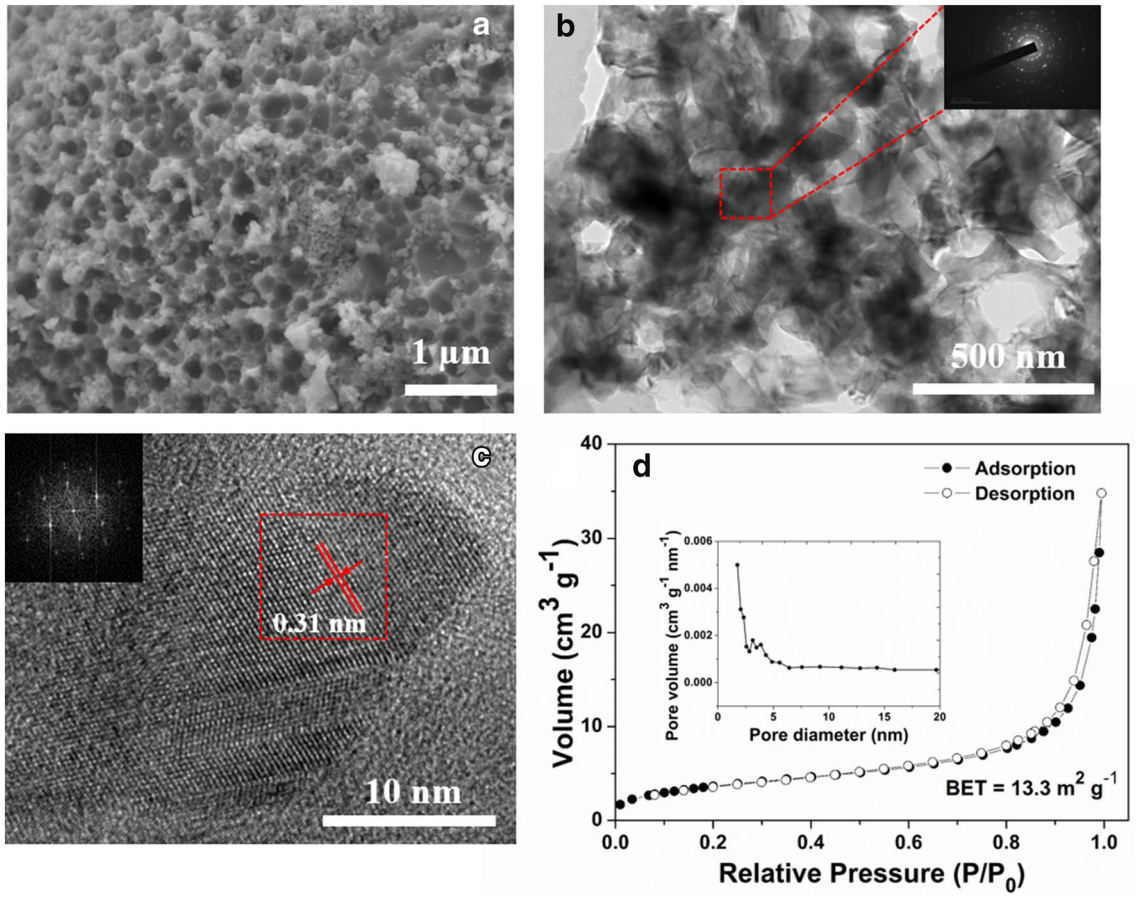

Fig. 4 Transformation of Nano-SiO_2 to Nano-Si. **a** SEM image of Nano-Si synthesised through magnesiothermic reduction of fly ashes-derived Nano-SiO_2. **b** TEM image of Nano-Si, the inset is the SADP image. **c** HRTEM image of the Nano-Si particle, the inset also is the SADP image. **d** Nitrogen adsorption and desorption curves of Nano-Si derived from fly ashes. Inset, pore distribution

For electrochemical evaluation, unlike commercial Si powders, the Nano-Si derived from solid waste fly ashes have high functionality due to their nanostructure. It shows better electrochemical performance without any further modification and coating (Fig. 5). Cyclic voltammetry (CV) experiments during the first three cycles show delithiation and lithiation peaks at typical potentials of the reaction of Nano-Si (Fig. 5a). The lithiation peak of about 0.12 V have been ascribed to the amorphous Li_xSi formation. The delithiation peaks appearing at 0.34 V and 0.51 V have been associated with the phase transformation between amorphous Li_xSi and amorphous Si [19]. Representative galvanostatic charge–discharge curves of Nano-Si electrodes (derived from solid waste fly ashes) at different current densities are presented in Fig. 5b. At the current density 100 mA g^{-1}, the Nano-Si electrodes exhibited specific capacities of 3432.1 and 2756.6 mAh g^{-1} for the discharging and charging cycles, respectively. The irreversible capacity loss may be ascribed to the SEI layers formation on the surface of Nano-Si electrodes and the lost of some lithium ions accompanied with irreversible reactions. The cycle performance of Nano-Si electrodes (derived from fly ashes) were contrasted with that of electrodes obtained by commercial Si powders (Fig. 5c). For the Nano-Si electrodes prepared by fly ashes, the discharge capacity of 1017.5 mAh g^{-1} at the given current density 1000 mA g^{-1} was maintained after 100 cycles, with the Coulombic efficiency reaching 80.32% in the first cycle and 98% even after just 3 cycles, respectively. Obviously, the coulombic efficiency (CE) of Nano-Si prepared by fly ashes in the first cycle is 80.32%. Such excellent CE indicates that the porous structure makes it possible to form the stable SEI layer in the first cycle. However, the Si anodes prepared by commercial Si powders showed a discharging capacity of 3863 mAh g^{-1} during the first cycle, but after only 30 cycles at 1000 mA g^{-1}, the capacity decreased drastically to 86 mAh g^{-1} (even lower than the 372 mAh g^{-1} theoretical capacity of graphite). In Fig. S3, the SEM images of Si electrodes prepared by fly ashes and commercial Si powders before and after cycling are exhibited. After 100 cycles, the apparent size of Nano-Si particles increased to some extent, mainly due to the formation of

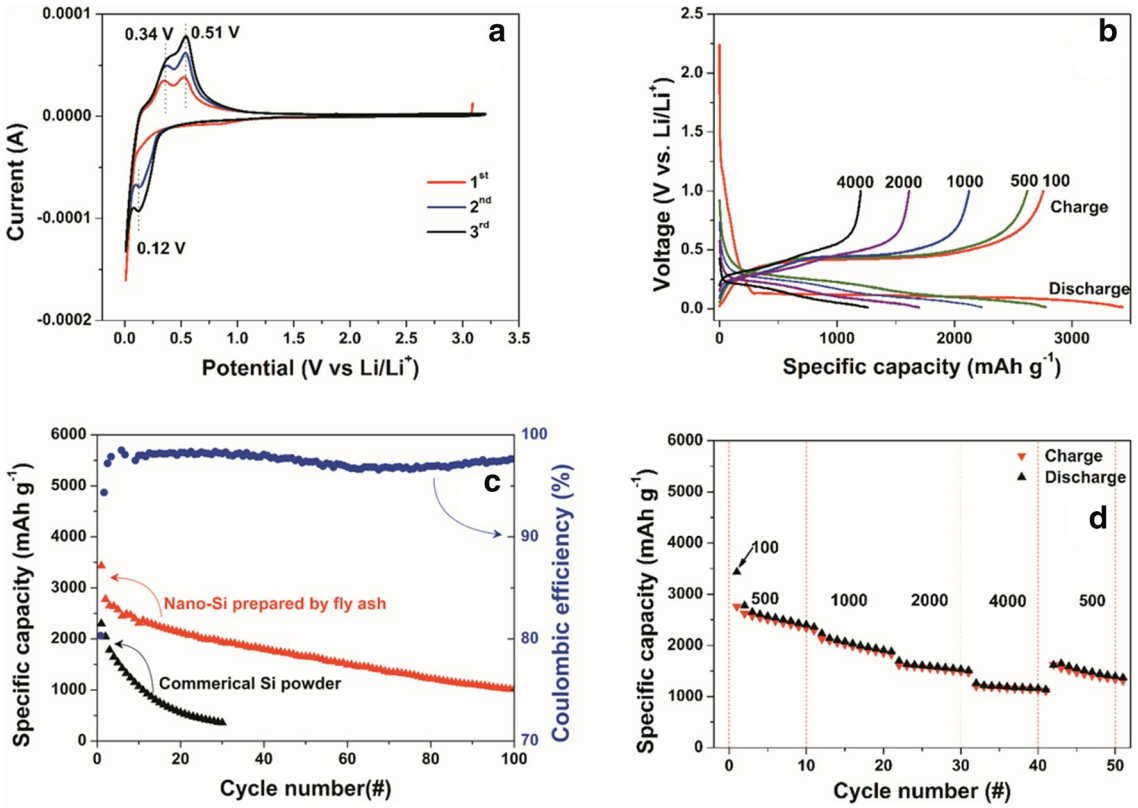

Fig. 5 Lithium-ion batteries anodes using Nano-Si derived from fly ashes. **a** Cyclic voltammogram (CV) versus Li/Li^+ by 0.02 mV s^{-1} scan in the first three cycles. **b** Gavanostatic discharge–charge curves at different current densities varying from 0.1 to 4 C (1C = 1000 mA g^{-1}). **c** Cycle performance of Nano-Si prepared by fly ashes and commercial Si powders electrodes. **d** Rate performance

SEI layers and irreversible volumetric expansion during the lithiation process. However, there are appreciable swelling and cracking for the commercial Si particles only after 30 cycles. The results proved that the Nano-Si particles could alleviate volume changes well concerned with the repeated lithiation-delithiation process. Also, the Nano-Si derived from fly ashes show good rate capacity (Fig. 5d). To evaluate it, the rate capability of the Nano-Si anodes (recovered from fly ashes) at different discharging rates are shown (Fig. 5d). The reversible capacities of 2792.5, 2112.0, 1571.6, and 1450.3 mAh g^{-1} were obtained at different discharging rates of 500, 1000, 2000, and 4000 mA g^{-1}, respectively. These values are 7.5, 5.7, 5.0, and 4.2 times more than the 372 mAh g^{-1} theoretical capacity of graphite, respectively.

4 Conclusion

The present study demonstrates that fly ashes, major solid waste by-products generated in coal-fired power plants, can be applied to synthesis Nano-Si with the porous structure as LIBs anodes. The Nano-Si derived from fly ashes can solve the key issues existing in Si anodes, showing excellent rate and cycling performance. In consideration of annual enormous supply of fly ashes on a global scale, this work show how the solid wastes, fly ashes, can be available resources that contribute to meeting the growing demand for Nano-Si materials in LIBs batteries.

Acknowledgements We acknowledge the financial supports from the Project Foundation of Chongqing Municipal Education Committee under Grant No. KJ1601338, the National Natural Science Foundation of China (51472037) and Shenzhen Science and Technology Innovation Committee (JCYJ20170818160815002). We thank Material Analysis and Testing Center of Chongqing University of Science and Technology for the help with all analysis and characterization.

Compliance with ethical standards

Conflict of interest The authors declare that they have no conflict of interest.

References

1. Shigemoto N, Hayashi H, Miyaura K (1993) Selective formation of Na-X zeolite from coal fly ash by fusion with sodium hydroxide prior to hydrothermal reaction. J Mater Sci 28:4781–4786
2. Burnard K, Bhattacharya S (2011) Power generation from coal. IEA Energy Pap
3. Bukhari SS, Behin J, Kazemian H, Rohani S (2015) Conversion of coal fly ash to zeolite utilizing microwave and ultrasound energies: a review. Fuel 140:250–266
4. Chandra N, Sharma P, Pashkov GL, Voskresenskaya EN, Amritphale SS, Baghel NS (2008) Coal fly ash utilization: low temperature sintering of wall tiles. Waste Manage 28:1993–2002
5. Nhan CT, Graydon JW, Kirk DW (1996) Utilizing coal fly ash as a landfill barrier material. Waste Manage 16:587–595
6. McCarthy GI (2011) X-Ray Powder Diffraction For Studying the Mineralogy of fly ash. MRS Proceedings 113
7. Fukasawa T, Karisma AD, Shibata D, Huang A-N, Fukui K (2017) Synthesis of zeolite from coal fly ash by microwave hydrothermal treatment with pulverization process. Adv Powder Technol 28:798–804
8. Aldahri T, Behin J, Kazemian H, Rohani S (2016) Synthesis of zeolite Na-P from coal fly ash by thermo-sonochemical treatment. Fuel 182:494–501
9. Khatri C, Rani A (2008) Synthesis of a nano-crystalline solid acid catalyst from fly ash and its catalytic performance. Fuel 87:2886–2892
10. Jain D, Khatri C, Rani A (2011) Synthesis and characterization of novel solid base catalyst from fly ash. Fuel 90:2083–2088
11. Majchrzak-Kucęba I (2012) Thermogravimetry applied to characterization of fly ash-based MCM-41 mesoporous materials. J Therm Anal Calorim 107:911–921
12. Mor S, Manchanda CK, Kansal SK, Ravindra K (2017) Nanosilica extraction from processed agricultural residue using green technology. J Clean Prod 143:1284–1290
13. Mor S, Chhavi MK, Sushil KK, Ravindra K (2018) Assessment of hydrothermally modified fly ash for the treatment of methylene blue dye in the textile industry wastewater. Environ Dev Sustain 20:625–639
14. Nakato Y, Shioji M, Tsubomura H (1981) Photovoltage and stability of an n-type silicon semiconductor coated with metal or metal-free phthalocyanine thin films in aqueous redox solutions. J Phys Chem 85:1670–1672
15. Cui Y, Lieber CM (2001) Functional nanoscale electronic devices assembled using silicon nanowire building blocks. Science 291:851–853
16. Lin VS-Y, Motesharei K, Dancil K-PS, Sailor MJ, Ghadiri MR (1997) A porous silicon-based optical interferometric biosensor. Science 278:840–843
17. Park J-H, Gu L, von Maltzahn G, Ruoslahti E, Bhatia SN, Sailor MJ (2009) Biodegradable luminescent porous silicon nanoparticles for in vivo applications. Nat Mater 8:331
18. Tian B, Cohen-Karni T, Qing Q, Duan X, Xie P, Lieber CM (2010) Three-dimensional, flexible nanoscale field-effect transistors as localized bioprobes. Science 329:830–834
19. Kovalenko I, Zdyrko B, Magasinski A, Hertzberg B, Milicev Z, Burtovyy R, Luzinov I, Yushin G (2011) A major constituent of brown algae for use in high-capacity Li-ion batteries. Science 334:75–79
20. Wu H, Chan G, Choi JW, Ryu I, Yao Y, McDowell MT, Lee SW, Jackson A, Yang Y, Hu L, Cui Y (2012) Stable cycling of double-walled silicon nanotube battery anodes through solid–electrolyte interphase control. Nat Nanotechnol 7:310
21. Li J-Y, Xu Q, Li G, Yin Y-X, Wan L-J, Guo Y-G (2017) Research progress regarding Si-based anode materials towards practical application in high energy density Li-ion batteries. Mater Chem Front 1:1691–1708
22. Luo W, Chen X, Xia Y, Chen M, Wang L, Wang Q, Li W, Yang J (2017) Surface and interface engineering of silicon-based anode materials for lithium-ion batteries. Adv Energy Mater 24:1701083
23. Dunn B, Kamath H, Tarascon J-M (2011) Electrical energy storage for the grid: a battery of choices. Science 334:928–935
24. Hu Y-S, Demir-Cakan R, Titirici M-M, Müller J-O, Schlögl R, Antonietti M, Maier J (2008) Superior storage performance of a Si@SiOx/C nanocomposite as anode material for lithium-ion batteries. Angew Chem Int Ed 47:1645–1649
25. Chan CK, Peng H, Liu G, McIlwrath K, Zhang XF, Huggins RA, Cui Y (2007) High-performance lithium battery anodes using silicon nanowires. Nat Nanotechnol 3:31
26. Yoshio M, Wang H, Fukuda K, Umeno T, Dimov N, Ogumi Z (2002) Carbon-coated Si as a lithium-ion battery anode material. J Electrochem Soc 149:A1598–A1603
27. Wu H, Cui Y (2012) Designing nanostructured Si anodes for high energy lithium ion batteries. Nano Today 7:414–429
28. Liu Z, Chang X, Wang T, Li W, Ju H, Zheng X, Wu X, Wang C, Zheng J, Li X (2017) Silica-derived hydrophobic colloidal nano-Si for lithium-ion batteries. ACS Nano 11:6065–6073
29. Liu Z, Chang X, Sun B, Yang S, Zheng J, Li X (2017) Room temperature solvent-free reduction of $SiCl_4$ to nano-Si for high-performance Li-ion batteries. Chem Commun 53:6223–6226
30. Jung DS, Ryou M-H, Sung YJ, Park SB, Choi JW (2013) Recycling rice husks for high-capacity lithium battery anodes. P Natl Acad Sci USA 110:12229–12234
31. Liu N, Huo K, McDowell MT, Zhao J, Cui Y (2013) Rice husks as a sustainable source of nanostructured silicon for high performance Li-ion battery anodes. Sci Rep 3:1919
32. Xing A, Tian S, Tang H, Losic D, Bao Z (2013) Mesoporous silicon engineered by the reduction of biosilica from rice husk as a high-performance anode for lithium-ion batteries. RSC Adv 3:10145
33. Liu J, Kopold P, van Aken PA, Maier J, Yu Y (2015) Energy storage materials from nature through nanotechnology: a sustainable route from reed plants to a silicon anode for lithium-ion batteries. Angew Chem Int Ed 54:9632–9636
34. Jiang Y, Zhang Y, Yan X, Tian M, Xiao W, Tang H (2017) A sustainable route from fly ash to silicon nanorods for high performance lithium ion batteries. Chem Eng J 330:1052–1059
35. Bao Z, Weatherspoon MR, Shian S, Cai Y, Graham PD, Allan SM, Ahmad G, Dickerson MB, Church BC, Kang Z, Abernathy Iii HW, Summers CJ, Liu M, Sandhage KH (2007) Chemical reduction of three-dimensional silica micro-assemblies into microporous silicon replicas. Nature 446:172